Six-axis vibration isolation technology applied to spaceborne interferometers

John F. O'Brien, Gregory W. Neat, James W. Melody, Robert J. Calvet

Jet Propulsion Laboratory, California Institute of Technology, Pasadena, CA

Andreas von Flotow

Hood Technology Corporation, Hood River, OR

ABSTRACT

This paper discusses the vibration isolation problem as it applies to spaceborne interferometers, and presents evidence that vibration isolation will be a required technology for these instruments. A hardware solution to the spaceborne interferometer isolation problem is offered with experimental evidence of its effectiveness.

Key Words: vibration isolation, precision pointing, Micro-Precision Interferometer, multi-layer control, IMOS.

1. INTRODUCTION

Spaceborne interferometers will provide high astrometric accuracy with significant mass savings over full aperture systems. Figure 1 is a simplified diagram of a spaceborne interferometer. The instrument collects light from a single stellar target using collecting optics that are separated by the length of the instrument structure. Light from both sides of the instrument is reflected off a like number of surfaces, and is combined at the beam combiner, where an interference fringe pattern is constructed. The interfered light is sampled by the fringe detector, and astrometric information concerning the target star is extracted. For a more in-depth discussion of optical interferometry, the reader is directed to Ref. 1.

There are two types of errors which affect spaceborne interferometer fringe visibility: wavefront tilt, and optical path difference (OPD) error. Wavefront tilt occurs when light reflected from one edge of a surface arrives at the beam combiner at a different time than the light reflected from the other edge of the same surface.[1] Interference fringe visibility is reduced because light from a single wavefront is not present at the combining optics at the same time. OPD error occurs when the distance travelled by the stellar light from the target star to the beam combiner through one side of the interferometer is different than the distance travel led through the other side. These errors have static (due to instrument pointing errors) and dynamic (due to structural vibrations) components. This paper focuses primarily on the effects of dynamic errors.

Sources ofvibration (for example, the reaction wheel assembly (RWA)) attached to the space interferometer will tend to drive the lightly damped resonances of the instrument structure. These vibrations will disturb the optical path, causing dynamic wavefront tilt and OPD errors. The Control Structure Interaction (CSI) team at JPL has developed a multi-layer control strategy to maintain sufficient fringe visibility in spite of these structurally amplified vibrations. The first control layer is optical control, where fast steering mirrors and active delay lines are used in high bandwidth disturbance rejection control systems to correct wavefront tilt and OPD errors, respectively.[2]. The optical control layer is very effective at low frequency, however, lightly damped modes of the spacecraft structure tend to couple destructively with the controllers at higher frequencies.

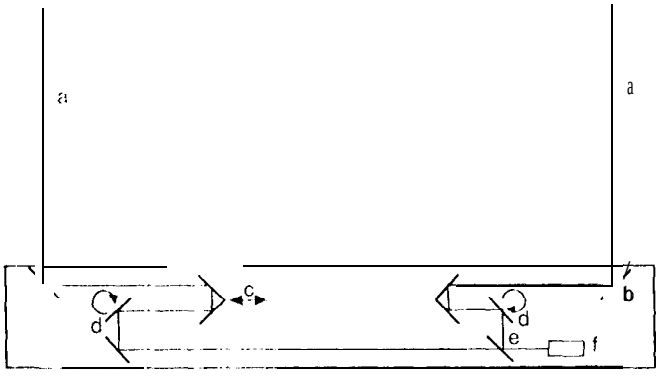

a. I IGHT FROM TH E SAME: STAR d. FAST STEERING MIRRORS
b. (COLLECTING OPTICS e. BEAM COMBINER
c. ACTIVE DELAY LINE. f. FRINGE DETECTOR

Fig. 1. A simplified diagram of a spaceborne interferometer.

To combat the effect of control-structure interaction, elements Of the structure arc replaced in strategic locations by damping devices to attack plant resonances that tend to reduce the amount of feedback available to the optical control systems. Structural damping elements can either be passive[3] or active[4] Structural damping has the added effect of reducing the net vibration level of the spacecraft, but this is of less importance than "treating" the optical controller plant. With the structural control layer in place, the unavoidable effects of photon count, digital sampling delay, and optical actuator resonances set the optical controller bandwidth limit (typically between 100 Hz and 1. kHz).

To attenuate wavefront tilt and OPD errors remaining after the optical and structural layers are implemented, sources of vibration (RWAs) are separated from the instrument by a vibration isolation system. The torque transmission of an ideal RWA isolation system is shown in Fig. 2.[5] The ideal isolator provides a rigid connection between the RWA and the spacecraft over the bandwidth of the attitude control system (ACS), and provides an infinitely compliant connection at higher frequencies, where unwanted reaction wheel harmonics reside. This isolation system would be quite difficult to realize.

One method of providing realizable vibration isolation is to suspend the RWA on soft springs. The torque transmission for a soft suspension is shown in Fig 3. Vibration amplification due to the "(bounce" mode of the suspension is undesirable, and can be attenuated through the application of a damping agent to the suspension system.

Another isolation method is to separate the RWA and the spacecraft by a mount consisting of stiff actuators and sensors. Broadband feedback can be implemented in an attempt to artificially realize the torque transmission of the ideal mount, but this would be difficult to achieve due to stability issues related to the large feedback requirement.[5] Narrowband feedback can be used to "notch out" torque transmission at the eigen-frequencies of critical structural modes. Narrowband tracking filters can be employed to follow RWA harmonics as the wheel speed changes. The torque transmission for the stiff actuator mount using narrowband feedback is shown in Fig. 4.

The vibration isolation capability of the soft mount can be enhanced by the presence of either stiff actuators in series with the springs (Fig. 5), or soft actuators in parallel with the springs (Fig. 6). Broadband feedback could be used to artificially reduce the bounce mode frequency of a moderately stiff suspension system, and hence increase isolation performance. Narrowband feedback could be implemented to increase the "(passive" isolation performance at critical frequencies. Figure 7 shows the torque transmission of the soft suspension with active augmentation.

Several vibration isolation systems have already been developed. Intelligent Automation, Inc. has constructed and tested a 6-degree-of-freedom (dof) *active* isolator using stiff Terfenol-D magnetostrictive actuators.[6] An RWA isolation system using lossy springs (viscous fluidic dampers) was built by Honeywell, Inc., and flown on the Hubble Space Telescope.[7] The CSI team at JPL has developed narrowband tracking isolation control systems using a soft, single-do f voice coil actuator.[8] A discussion of the JPL CSI 6-dof vibration isolation system appears later in this text.

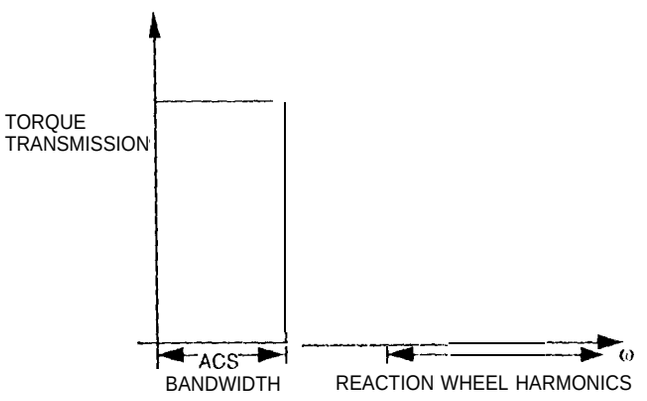

Fig. 2. Torque transmission for an ideal isolator.

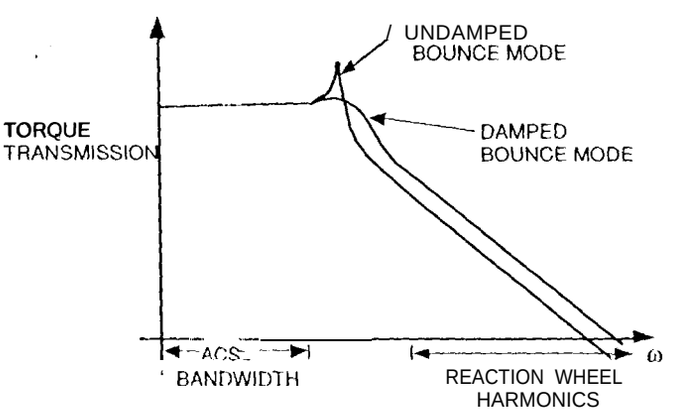

Fig. 3. Torque transmission for a soft suspension.

2. SPACEBORNE INTERFEROMETER ISOLATION PROBLEMS

Proposed spaceborne interferometers can be segregated into two types based on the relative location of the vibrating sources and the desired quiet components.

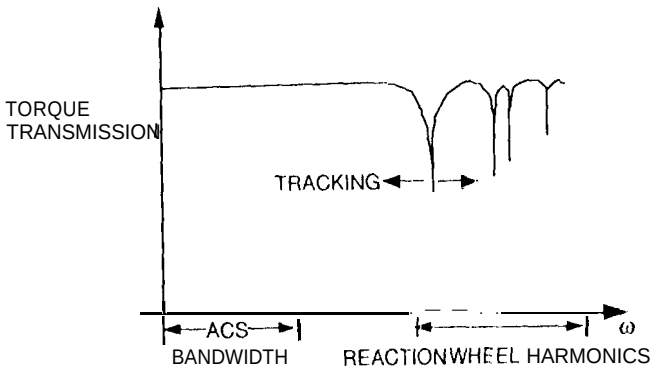

Fig. 4. Torque transmission for an active isolator using narrow band feedback on stiff actuators,

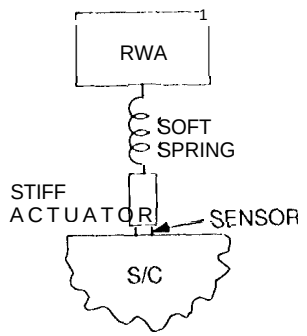

Fig. 5. Soft suspension with active augmentation : stiff actuator in series with a soft spring.

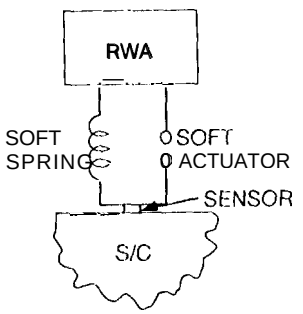

Fig. 6. Soft suspension with active augmentation: soft actuator in parallel with a soft spring.

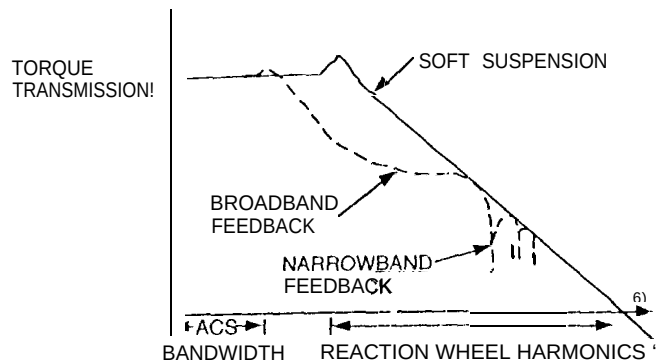

Fig. 7. Torque transmission for a soft suspension with active augmentation.

2.1 Noisy box interferometers

Noisy box interferometers are typified by discrete optical components distributed across a long spacecraft structure. An example of a noisy box interferometer is the Orbiting Stellar Interferometer (0 S1)[9], shown in Fig. 8. These instruments employ high bandwidth, high dynamic range optical disturbance rejection control systems to attenuate both OPD and wavefront tilt errors. Some noisy box interferometers utilize articulating collecting optics to feed stellar light into the instrument.. This reduces the attitude control system requirement of precisely pointing the entire spacecraft at the target star.

The isolation system task applied to noisy box interferometers is to attenuate vibration transmission from the noisy box (RWA) to the quiet spacecraft structure, primarily at high frequency where the optical control systems lose effectiveness. Figure 9 shows a simplified diagram of the noisy box interferometer isolation problem.

Other examples of noisy box interferometers are the Laser Stabilized Imaging Interferometer (LASII)[10], and the Si nail 0S1 for Narrow-angle Astrometry with Two Apertures (SONATA). [11]

2.2 Quiet box interferometers

The quiet box interferometer is characterized by a self-contained instrument attached to a spacecraft bus. In contrast to the noisy box interferometer, this instrument does not employ high bandwidth optical disturbance rejection control systems or articulating collecting optics. Figure 10 is a diagram of the F'recision Optical

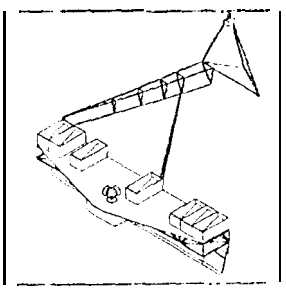

Fig. 8. Orbiting Stellar Interferometer (OSI).

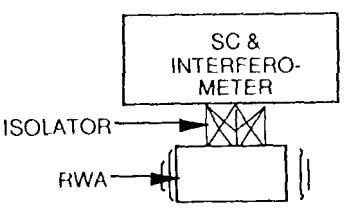

Fig. 9. Noisy Box Interferometer Isolation Problem.

Fig. 1(1. Precision Optical INTerferometer in Space(POINTS).

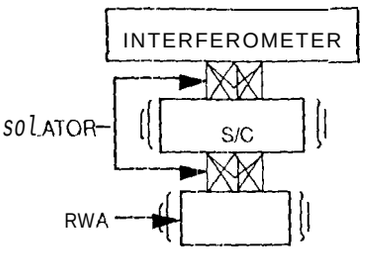

Fig. 11. Quiet box interferometer isola tion problem.

INTerferometer in Space (POINTS)[12], a quiet box interferometer.

The isolation system task for quiet box interferometers is to attenuate disturbance transmission from the vibrating spacecraft structure into the quiet box (interferometer). Additionally, the isolation system may be required to provide a precision pointing functionality to augment the accuracy of the spacecraft attitude control system. The quiet box interferometer may also employ a second isolation system to attenuate disturbance t ransmission from the RWA to the spacecraft bus, as in the noisy box problem. Figure 11 shows a diagram of the quiet box interferometer isolation problem.

Another example of a quiet box interferometer is the Smithsonian Astrophysical Observatory's Newcomb.[13]

3. REQUIREMENTS DISCUSSION

This section will discuss interferometer fringe visibility loss as a function of OPD stability and instrument pointing accuracy. Wavefront tilt errors also cause fringe visibility loss, but the stability requirement tends to be less stringent than that of OPD[1], and thus will not be addressed in this paper.

3.1 OPD stability

Maximum acceptable fringe visibility loss due to OPD vibrations is assumed to be 1%. From Colavita,[14]

$$V = e^{-\sigma_{opd}^2/} \quad (1)$$

From eqn. 1, an OPDjitter (σ_{opd}) of 0.14 radians, rms results in a fringe visibility(V) of 99%. Assuming an average stellar wavelength of 0.55 μm (visible light), this corresponds to a *maximum allowable OPD vibration of 12 nm, rms.* This is a fairly standard OPD stability value; it is applicable to many proposed spaceborne interferometers.

3.2 Pointing accuracy

Quiet box interferometers do not employ articulating collecting optics. Thus, the entire instrument must be precisely pointed at the stellar target. From Ref. 15, the required pointing accuracy for the POINTS instrument is 5 nanoradians. Since the POINTS attitude control system deadband will likely be greater than 5 nanoradians, the instrument will require a fine pointing system to augment ACS pointing accuracy.

4. ANALYTICAL. MODEL 1)ESCRIPTION

To quantify the expected OPD jitter due to RWA harmonics for both noisy (SONATA) and quiet box (POINTS) interferometers, models of both systems were developed using the Integrated Modelling of Optical Systems (IMOS) software package.[16] IMOS is a powerful analytical tool that operates in a MATLAB environment, and allows the generation of models that includes the effects of optical, structural, and control parameters.

4.1 RWA disturbance model

The RWA disturbance model actually consists of three separate models: a radial force model, a radial torque model, and an axial force model. These three models are used to generate five disturbance spectra: two radial forces, two radial torques, and an axial force. In developing, the RWA models, an attempt was made to capture the effect of slight variations in the wheel speed. To accomplish this, a stochastic distu rbance model was derived by assuming that the wheel speed is a uniform random variable over a small interval [Ro - dR/2, Ro + dR/2], where dR is the

expected wheel speed deviation about the wheel bias speed Ro. The result of this assumption is that the RWA disturbances are stochastic processes with power spectra that no longer exist only at discrete frequencies.

4.2 **Finite clement structural models**

130th the POINTS and SONATA structures were modelled using finite elements. The finite element model of POINTS uses beam elements (modelling axial, bending, and torsional stiffness). The POINTS model has 64 nodes and 360 dofs. The SONATA finite element model uses both beam elements and plate elements, resulting in 79 nodes and 378 dofs. For each model, a uniform modal damping of O. 1% was assumed.

4.3 **Optical models**

The linear optical models were generated from differential ray traces based on the physical optical prescription of each of the optical systems. The optical prescriptions consist of opt ical element positions and orientations specified in three-dimensional space (relative to the structure), and descriptions of the shape of the optical elements (focal length and eccentricity). From these optical prescriptions, the partial derivatives of the geometric ray trace with respect to element positions and orientations are generated. 'I'he linear optical models will then yield optical path difference as a function of optical element positions. ,

The structural and optical models are then combined, and since they are both linear, the combined model is be used to generate five transfer functions from the five different RWA disturbances to OPD.

5. **ANALYTICAL MODEL RESULTS—SONATA**

Figure 12 shows five RWA PSDs, the corresponding transfer functions to OPD, and the resulting OPD I'SD. This analytical data represents the worst case combination of reaction wheels and interferometers (the wheel with the largest coupling to one of the four SONATA interferometers). For this case, the reaction wheel speed is 1805 RPM, with an interval width of 50 RPM.

Shown with the OPD PSD is the cumulative rms. This function visually indicates where the maximum allowable OPD is breached, in this case at about .85 Hz. The resulting rms OPD is 136 nm, rms, which results in a fringe visibility loss of 70%.

SONATA is a noisy box interferometer, and thus will employ a pathlength control system for each of its four interferometers. However, the bandwidth of this control system will be about 100 Hz. The model indicates the presence of many resonances beyond 100 Hz that if driven by reaction wheel harmonics, as in this particular case,

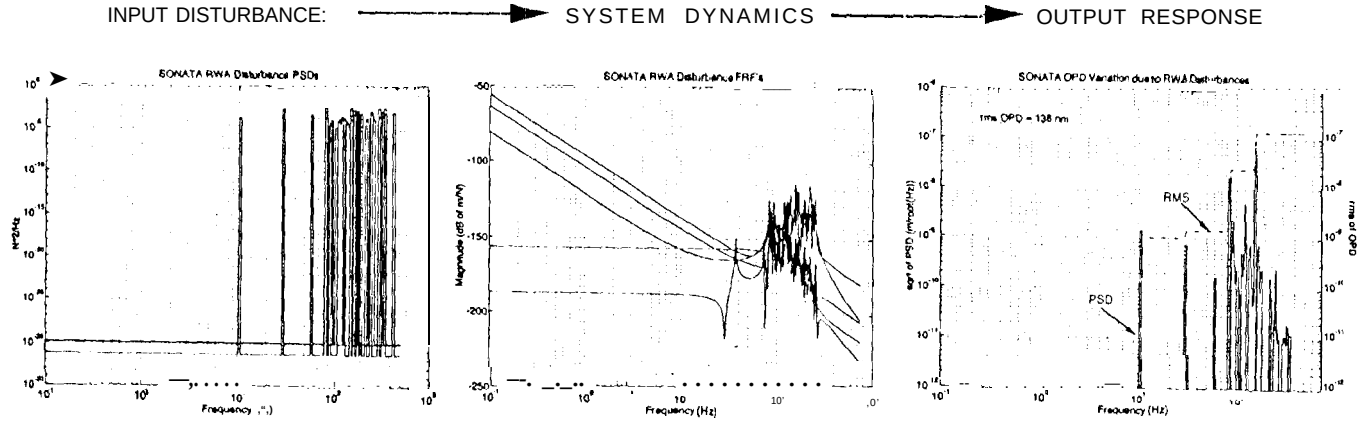

Fig. 12. SONATA IMOS model t esults.

will cause OPD vibrations far in excess of the defined maximum allowable value. For this reason, SONATA will likely require a vibration isolation system for its RWA.

6. ANALYTICAL MODEL RESULTS—POINTS

The same strategy was used to generate OPD jitter predictions for the POINTS instrument. A worst case combination was again chosen for this exercise (the worst coupling of one of the three modelled reaction wheels with one of the two POINTS interferometers). Figure 13 shows a specific case where the wheel speed is 2547 RPM, ± 25 RPM. The modal environment of the POI NJ'S instrument is significantly less dense than SONATA, however there are several structural resonances in the 10 to 100 Hz decade that, if driven by RWA harmonics will produce sizable OPD jitter, as seen in this case where the resulting OPD is 77 1 nm, rms. From Eq. 1., this translates to a nearly complete loss of fringe visibility due to OPD vibrations. As a quiet box interferometer, POINTS will not employ dynamic pathlength control systems, thus an isolation system for this instrument will be mandatory.

7. A SOLUTION—SASSIE

The design of the JPL six-axis vibration isolation / precision-pointing system was influenced by several different factors, In light of the IMOS predictions, the ability of the isolation system to provide performance in the event of an active system failure was heavily weighted. Thus, a completely active, stiff actuator isolation system was not considered appropriate. A trade study was performed comparing soft suspension isolators that retained active augmentation capabilities. The trade space is shown in Fig. *14.* There was an effort to avoid actuation systems that required exotic power supplies that would be difficult to implement in flight hardware. Hence, stiff actuators (piezoelectric and electrostrictive) in series with soft springs were considered less attractive alternatives to soft actuators (voice-coils) in parallel to soft springs. Eventual] y, voice coils were chosen for the isolator struts due to their driver electronics simplicity, low cost, and analyzability.

JPL, Hood Technology Corp., and Payload Systems, Inc. are currently developing the Six-Axis Smart Strut Isolation Experiment (SASSIE) isolation system, which will provide a solution to both the noisy and quiet box interferometer isolation design problems. The SASSIE isolator is a 6-dof soft suspension with active augmentation. A photograph of prototype SASSIE hardware is shown in Fig. 15.

Each of the six struts shown in Fig. 15 contains a voice coil in parallel to two soft diaphragm flexures. The axial compliance of each of the struts is sufficient to place the modes of the hexapod approximately within the octave between 20 and 40 Hz. Passive isolation performance in six degrees of freedom is provided at frequencies beyond 40 Hz. SASSIE isolators used in space will have hexapod eigenvalues a decade lower than this, but the problems associated with very soft suspensions in 1 g compelled a stiffer suspension for the prototype isolator. Each strut contains a force sensor located between the voice coil armature and a cross-blade flexure at the base of the strut. Inertial sensors can be attached to the isolator to supplement or replace the force sensors. The voice coils and sensors

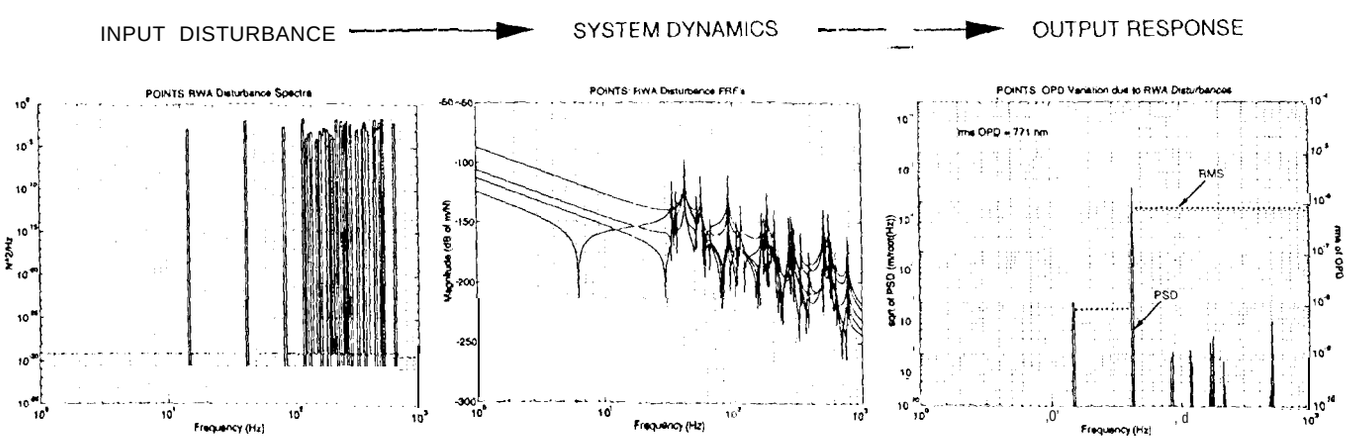

Fig. 13. POINTS *IMOS model results.*

are used in closed loop control systems to augment the isolation performance of the soft suspension. The voice coils can also be used in conjunction with an optical sensor mounted on the isolator to provide a precision-pointing functionality that is applicable to the quiet box interferometer problem, The six struts are arranged in a mutually orthogonal hexapod. This configuration reduces geometric coupling between actuators, thus making the control problem more tractable. It also provides a standardized architecture that applies to many proposed missions without significant modification, resulting in "off-the-shelf" cost savings.

8. NOISY BOX ISOLATOR VALIDATION

The JPL Micro-Precision Interferometer (MPI) is a functional, ground-based model of a spaceborne interferometer[17] The MPI structure consists of three flexible truss booms that converge at a vertex where sources of vibration are attached. A noisy box interferorneter, MPI has discrete optical components distributed across the truss structure. It has high bandwidth optical actuators that are used in disturbance rejection control systems to reduce dynamic wavefront tilt and OPD errors. Articulating collecting optics feed light into the instrument from a simulated stellar source.

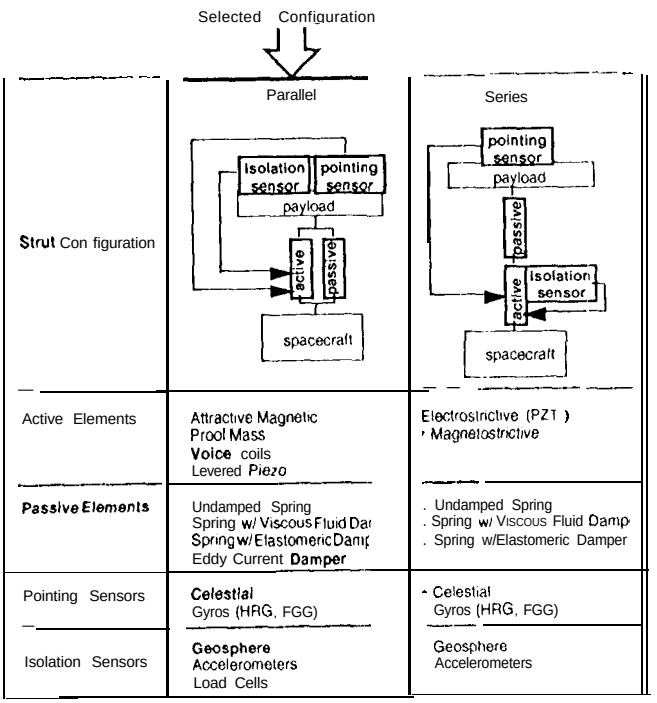

Fig. 14. JPL isolator trade space.

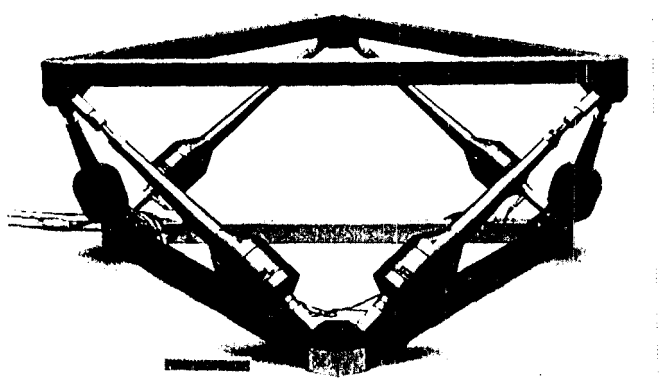

Fig. 15. Prototype SASSIE 6-axis isolator.

To fulfill its function as a testbed, MPI must provide a dynamic environment that is comparable to the actual flight systems that it simulates. A transfer function of input disturbance force to OPD experimentally acquired from the MPI testbed is compared to an IMOS prediction of the same transfer function for the SONATA instrument in Fig. 16. Note that the backbone of the transmission functions are comparable, indicating that MPI adequately synthesizes a spaceborne interferometer dynamic environment.

Initial isolation experiments have been performed using the prototype SASSIE isolator on the MPI testbed in the dirty box configuration depicted in Fig. 17. The performance metric for the experiment is the transfer function of a broadband input force (provided by a mini-shaker mounted in the vertex of the MPI structure) to

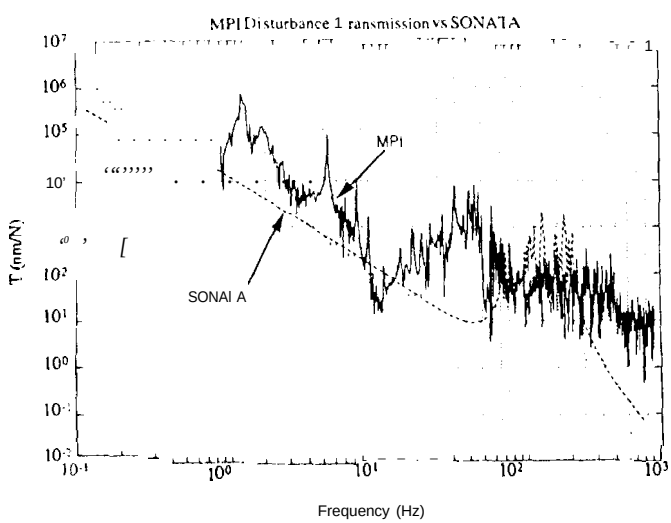

Fig. 16. Vibration transmission function comparison: MPI (solid) vs. SONATA (dashed).

Fig. 17. Prototype SASSIE isolator mountedon MPI

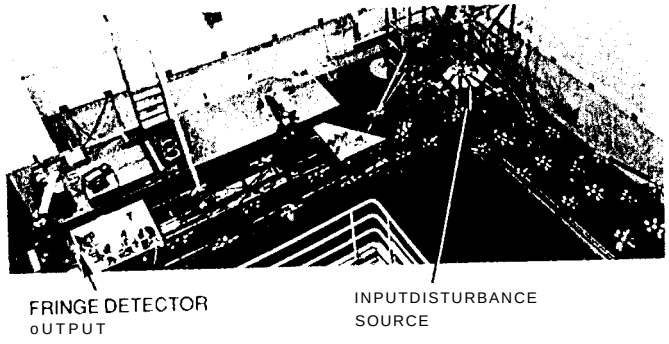

Fig. 18. Isolation experiment set-up on MPI

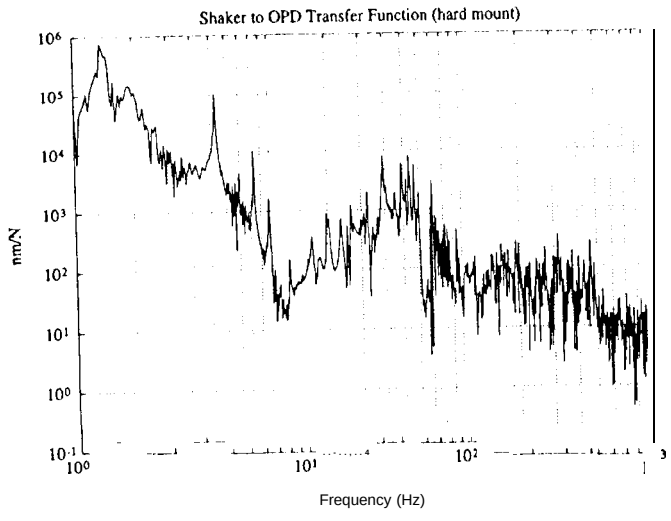

Fig.19. Disturbance to OPD transfer function on MPI: shaker rigidly mounted

OPD jitter (measured bytheinstrument fringe detector) depicted in Fig. 18. This transfer function with the shaker rigidly attached to the MPI structure is shown in Fig. 19.

The shaker was then mounted on the isolator, which provides a 6-axis soft suspension. The metric transfer functions for the rigidly mounted shaker and suspended shaker (passive isolation) from 100 - 900 Hz are compared in Fig. 20. The lack of transfer function coherence at high frequency is caused by the restricted amplitude capability of the shaker, coupled with the mass-like transin npedance of the MPI structure.

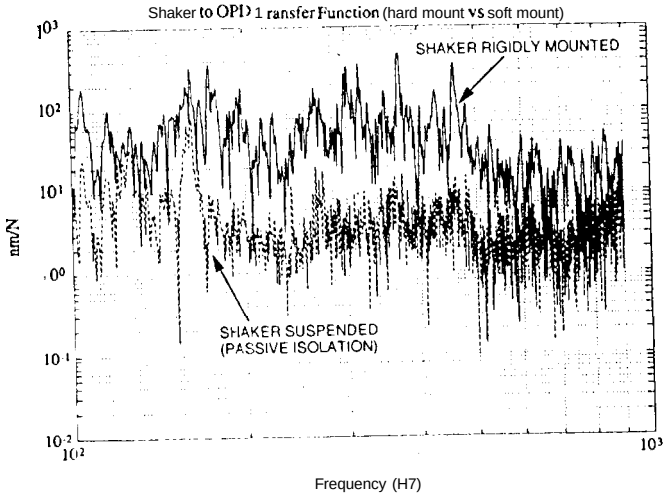

Fig. 20. Disturbance to OPD transfer function on MPI: shaker suspended on SASSIE hexapod

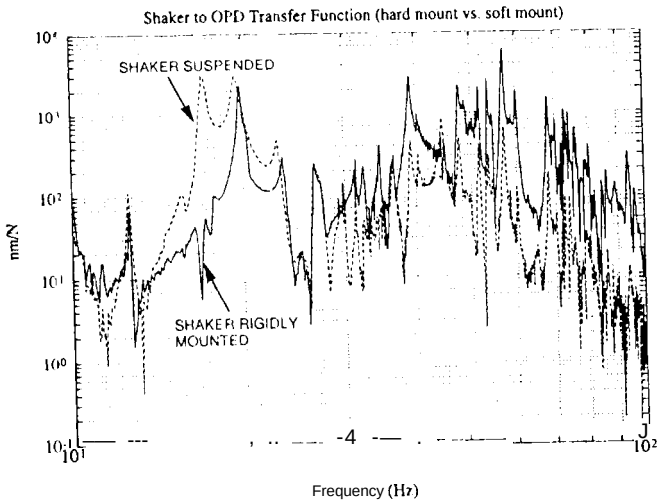

Fig. 21. Disturbance to OPD transfer function on MPI: shaker suspended on SA SSIE hexapod

Figure 21 shows the comparison of the same transfer functions at lower frequency, where the amplification of shaker vibrations by undamped isolator modes is made evident, This effect can be reduced by increasing the loss factor of the hexapod struts.

Six identical, broadband force feedback control systems using the hexapod actuators were closed to augment the passive isolation performance. 18 The effect of the active isolation system is evident in Fig. 22, where the passive isolation performance is compared to the passive isolation with active augment ation performance.

9. QUIET BOX ISOLATION/PRECISION-POINTING TECHNOLOGY DEVELOPMENT

The prototype SASSIE hexapod has been used in an isolation experiment on the MPI testbed in the quiet. box configuration. The reader is directed to Ref. 19 for a detailed description of the experiment.

In addition to the isolation functionality, POINTS also requires a pointing capability. In this case, command signals to the SASSIE actuators are derived from signals from both isolation and pointing sensors. The isolation loop rejects high frequency disturbances, while the pointing loop rejects low frequency disturbances. For the POINTS instrument, two pointing options exist. The first is the "nested" configuration, shown in Fig. 23. In this configuration, the reaction wheels serve both coarse and fine-pointing functions. Initially, the RWA adjusts the attitude of the spacecraft using information from the star tracker with sufficient accuracy to allow fringe observation from the bright star or guide interferometer. Astrometric information from the guide interferometer is then used to drive both the reaction wheels and the SASSIE pointing system to achieve very high pointing accuracy. By coupling the reaction wheels and the SASSIE pointing system with a common sensor, the nested pointing configuration allows the ACS to desaturate the SASSIE actuators. If the coarseness of the reaction wheels is sufficiently small, the ACS, with information from the interferometer, could be dedicated to the whole pointing task, and the SASSIE system could be dedicated only to vibration isolation. In this condition, a completely passive SASSIE isolator becomes an option. It is important to note that the nested pointing configuration is hinged on the assumption that the interferometer can be integrated with the ACS without a prohibitive cost increase.

The block diagram for the "stand- alone" pointing configuration is shown in Fig, 24, where the ACS and the SASSIE pointing system are decoupled. This architec-

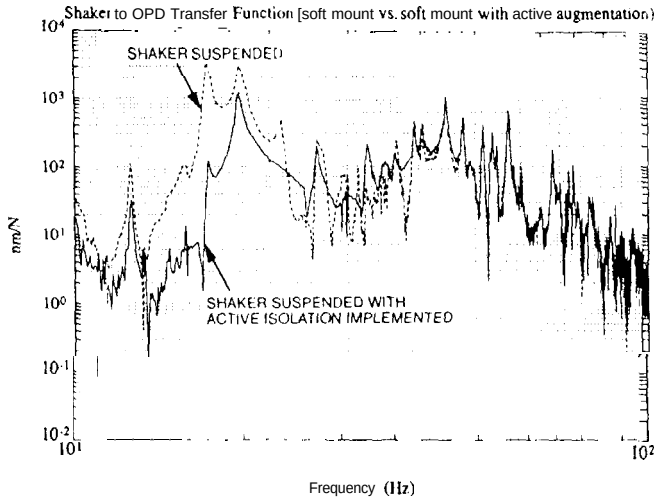

Fig. ?2. Disturbance to OPD transfer function on MPI: active isolation control system activated

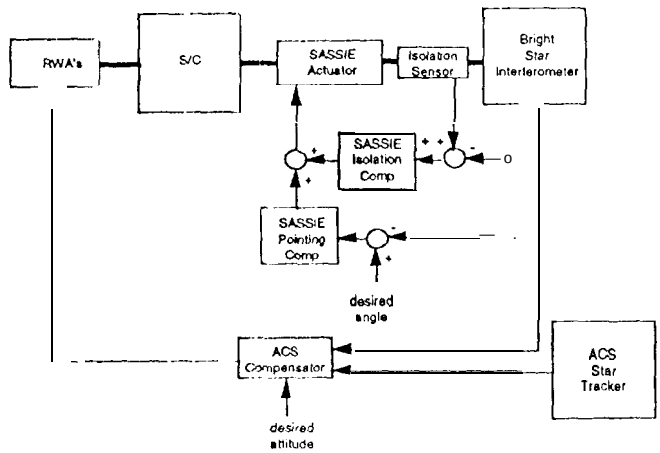

Fig. 2.?. Nested pointing configuration

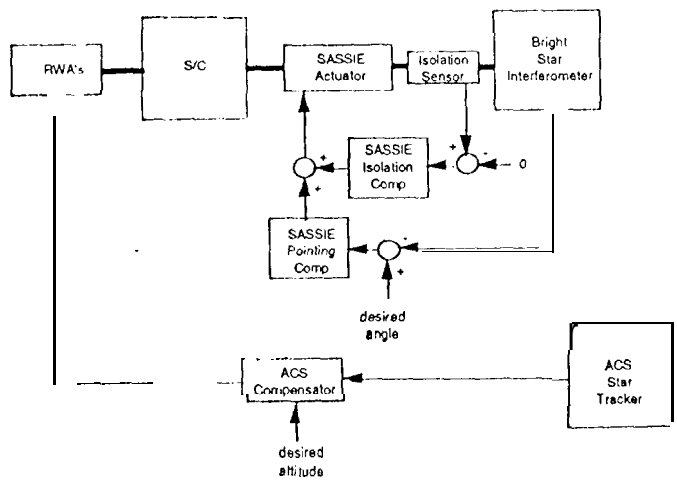

Fig. 24. Stand-alone pointing configuration

ture would be somewhat easier to integrate than the nested configuration. If the ACS is sufficiently accurate (e.g. 0.25 arcsec), the required stroke for the SASSIE pointing system will not be difficult to achieve.

10. CONCLUDING REMARKS

Analytical predictions indicate the presence of substantial OPD jitter due to RWA harmonics in frequencies beyond the bandwidth of the SONATA pathlength control system, resulting in a 70% loss of fringe visibility. To ensure adequate fringe visibility, the SONATA instrument should employ a vibration isolation system for its reaction wheel assembly.

An IMOS model of the POINTS instrument predicts significant RWA driven OPD jitter causing a nearly complete loss of fringe visibility. POINTS, a quiet box interferometer, will not have a dynamic optical control system, and thus will require an isolation system. Stringent instrument pointing requirements, coupled with the lack of articulating collecting optics, create the need for the POINTS isolation system to provide a precision-pointing functionality to relax ACS accuracy requirements.

SASSIE vibration isolation/precision-pointing technology provides a common solution to the quiet and noisy box interferometer isolation problems. Results from preliminary active isolation experiments performed on the MPI testbed using a prototype SASSIE isolator in the noisy box configuration show good vibration attenuation.

Future experiments with the prototype SASSIE hardware will include the development of a damping mechanism for the hexapod resonances, the design of a coupled multi-input, multi-output active isolation control system, the implementation of a precision, two-axis pointing system for application to the quiet box interferometer problem, and the isolation of flight traceable disturbances (a Magellan flight spare reaction wheel) on the MPI testbed. The knowledge and experience accumulated using the prototype SASSIE hardware will be put to use when a flight SASSIE isolator is developed for a validation test in the shuttle cargo bay.

11. ACKNOWLEDGE ENTS

The authors would like to thank the following for their contributions to this work: Johnny Carson, John Spanos, Stuart Shaklan, and Robert Laskin at JPL, and Marc Regelbrugge at Lockheed Palo Alto Research Laboratories. This research was performed at the Jet Propulsion Laboratory of the California Institute of Technology under contract with the National Aeronautics and Space Administration.

12. REFERENCES

1. G.H. Blackwood, R.N. Jacques, and D.W. Miller, "The MIT multipoint alignment testbed: technology development for optical interferornetry," SPIE Conference cm Active and Adaptive Optical Systems, July 1991.
2. J. Spanos, Z. Rahman, C-C. Chu, and J.F. O'Brien, "Control structure interaction in long baseline interferometers," 12th IFAC Symposium on Automatic Control in Aerospace, September 1992.
3. L.P. Davis, B.J. Workman, C.C. Chu, and E.H. Anderson, "Design of a D-Strut and its application results in the JPL, MIT, an LaRC test beds," ATAA SDM, April 1992.
4. J. J. O'Brien and G.W. Neat, "Automated tuning of active truss elements for application to spaceborne interferometers," 4th International Conference on Adaptive Structures, November 1993.
5. K.B. Scribner, L.A. Sievers, and A. von Flotow, "Active narrow band vibration isolation of machinery noise from resonant substructures," Journal of Sound and Vibration, Vol. 167, p. 17-40, 1993.
6. Z.J. Geng and L.S. Haynes, "Six degree-of-freedom active vibrat ion control using the steward platforms," IEEE Transactions on Control Systems Technology, Vol 2, No. 1, pp. 45-53, March 1994.
7. J J. Roddeb, H.J. Dougherty, L. F'. Reschke, M.D. Hasha, and L.P. Davis, "Line of sight performance improvement with reaction wheel isolation ," AAS Guidance and Control Conference, February 1986.
8. J. Spanos, and Z. Rahman, "Narrow-band control experiments in active vibration isolation," SPIE Conf. on Vibration Monitoring and Control, Vol. 2264, July 1994.
9. M.M. Colavita, M. Shao, and M.D. Rayman, "0S1: orbiting stellar interferometer for astrometry and imaging," Williamsburg Space Optics Conference, 1992.

10. R.T. Stebbins, P. I.. Bender, "Update on the laser-stabilized imaging interferometer," SPIE's Symposium on Aerospace/Defence Sensing & Control and Dual Use Photonics, April 1995.
11. J. Yu, M. Shao, M.M. Colavita, and M.D. Rayman, "Design of an orbiting stellar interferometer for planet detection," SPIE Symposium on Spaceborne Interferometry, Vol. 1947, April 1993.
12. R.D. Reasenberg, R.W. Babcock, M.A. Murison, M.C. Noecker, J.D. Phillips, B.J,. Schumaker, and J.S. Ulvestad, "POINTS: an astrometric spacecraft with multifarious a pplications," SPIE 'J'ethnical Conference on Amplitude and Intensity Spatial Intensity Spatial Interferornetry 11, Marcl 11994.
13. R. I). Reasenberg, R. W. Babcock, J. Il. Phillips, K.J. Johnston, and R.S. Simon, "Newcomb, a scientific interferometry mission at low cost," SPI E Technical Conference #2200, March 1994.
14. M.M. Colavita, "0S1 sensitivity, guide-star limiting magnitudes, and visibility reductions," JPL IOM, March 1992.
15. Private conversation with Robert Reasenberg.
16. H.C. Briggs, "Integrated modelling of optical systems guide...release 1.0," June 1992.
17. G.W. Neat, J.F. O'Brien, R.J. Calvet, H. Singh, and N.M. Nerheim, "Micro-precision interferometer testbed: initial stabilized stellar fringe results," SPIE Symposium on Aerospace/Defence Sensing & Control and Dual-Use Photonics, April 1995.
18. J. Spanos, Z. Rahman, and G. Blackwood, "A soft 6-axis active vibration isolator," American Control Conference, June 1995.